

Separation of CO₂ and H₂S Using Room-Temperature Ionic Liquid [bmim][MeSO₄]

Mark B. Shiflett,^{*,†} Anne Marie S. Niehaus,[†] and A. Yokozeki[‡]

DuPont Central Research and Development, Experimental Station, Wilmington, Delaware 19880, and 109-C Congressional Drive, Wilmington, Delaware 19807

We have developed a ternary equation of state (EOS) model for the CO₂/H₂S/1-butyl-3-methylimidazolium methylsulfate ([bmim][MeSO₄]) system to understand separation of these gases using room-temperature ionic liquids (RTILs). The present model is based on a modified RK (Redlich–Kwong) EOS, with empirical interaction parameters for each binary system. The interaction parameters have been determined using our measured VLE (vapor–liquid equilibrium) data for H₂S/[bmim][MeSO₄] and literature data for CO₂/[bmim][MeSO₄] and CO₂/H₂S. Due to limited VLE data for H₂S/[bmim][MeSO₄], we have also used VLLE (vapor–liquid–liquid equilibrium) measurements to construct the EOS model. The VLLE for H₂S/[bmim][MeSO₄] is highly asymmetric with a narrow (mole fraction H₂S between 0.97 and 0.99) LLE gap which is the first such case reported in the literature and exhibits Type V phase behavior, according to the classification of van Konynenburg and Scott. The validity of the ternary EOS model has been checked by conducting VLE experiments for the CO₂/H₂S/[bmim][MeSO₄] system. With this EOS model, solubility (VLE) behavior has been calculated for various (*T*, *P*, and feed compositions) conditions. For large (9/1) and intermediate (1/1) CO₂/H₂S feed ratios, the CO₂/H₂S gas selectivity is high (10 to 13, compared with <4.5 in the absence of ionic liquid) and nearly independent of the amount of ionic liquid added. For small CO₂/H₂S mole ratios (1/9) at 298.15 K, increasing the ionic liquid concentration increases the CO₂/H₂S gas selectivity from about 7.4 to 12.4. For high temperature (313.15 K) and large CO₂/H₂S feed ratios, the addition of the ionic liquid provides the only means of separation because no VLE exists for the CO₂/H₂S binary system without the ionic liquid.

Introduction

Hydrogen sulfide (H₂S) and carbon dioxide (CO₂) are commonly removed from natural and synthesis gases through chemical absorption using aqueous solutions of organic bases like single amines, amine mixtures, or mixtures of an amine and a salt of an amino acid.^{1,2} Extensive research has been conducted by several groups on aqueous solutions of alkanolamines, especially monoethanolamine (MEA), diethanolamine (DEA), and methyldiethanolamine (MDEA) for natural gas treating and sweetening.^{3–13} The typical process involves competitive chemical absorption of H₂S and CO₂ in a packed column at low temperature (preferably ambient temperature) and elevated pressures (up to about 4 MPa or more). The gas desorption or solvent regeneration occurs at elevated temperatures (typically around (350 to 400) K) and low pressures using a stripping column. Disadvantages of aqueous solutions of alkanolamines include loss of the amine during regeneration, transfer of water into the gas stream, degradation of the amine to form corrosive byproducts, high temperature required for desorption, and low temperature and high pressure absorption, all of which make this process economically expensive.

Room-temperature ionic liquids (RTILs) have been proposed for the capture of gases such as CO₂. Several solubility studies of CO₂ in RTILs have been reported;^{14–27} however, only a few researchers have examined the binary phase *PTx* (pressure–

temperature–composition) behavior of H₂S in ionic liquids.^{28–32} Jou and Mather²⁸ reported the first solubility data of H₂S in 1-butyl-3-methylimidazolium hexafluorophosphate ([bmim][PF₆]) at temperatures from (298.15 to 403.15) K and pressures up to 9.6 MPa. Pomelli et al.²⁹ measured the solubility of H₂S in different imidazolium-based ionic liquids with various anions and in a series of bis(trifluoromethyl)sulfonylimide (Tf₂N)-based ionic liquids with various cations at 298.15 K and 1400 kPa. Heintz et al.³⁰ attempted to measure the solubility of CO₂ and a mixture of N₂/H₂S in an ionic liquid with an ammonium cation and chloride anion from (300 to 500) K and pressures up to (0.23 and 3.0) MPa for H₂S and CO₂, respectively; however, the structure of the ionic liquid was unknown, and an approximate chemical formula was assumed for calculating the mole fraction solubilities.

Recently, Jalili et al.³¹ measured the solubility of H₂S in three RTILs ([bmim][PF₆], [bmim][BF₄], and [bmim][Tf₂N]) at temperatures from (303.15 to 343.15) K and pressures up to 1 MPa. In each case, the H₂S solubility is much higher than the CO₂ solubility. For example, Henry's law constants are (5.17 and 0.143) MPa at 298 K for CO₂ and H₂S in RTIL ([bmim][PF₆]), respectively.^{17,31} This large difference in Henry's law constant suggests that selective capturing and separation of these gases may be possible using ionic liquids. This motivated us to publish our first paper on the separation of CO₂/H₂S using the [bmim][PF₆] ionic liquid.³² We concluded that [bmim][PF₆] was not necessarily the best choice for the gaseous separation and/or capturing of CO₂ and H₂S. The selection was merely a demonstration of our method to measure and model ternary VLE

* To whom correspondence should be addressed. Phone: 302-695-2572. Fax: 302-695-4414. E-mail: mark.b.shiflett@usa.dupont.com.

[†] DuPont Central Research and Development, Experimental Station.

[‡] 109-C Congressional Drive.

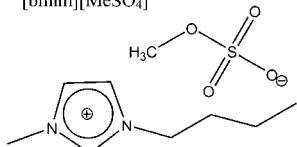
Chemical Name	Abbreviation	Structure
1-butyl-3-methylimidazolium methyl sulfate	[bmim][MeSO ₄]	

Figure 1. Chemical structure of [bmim][MeSO₄].

behavior. However, the ionic liquid did affect the gaseous selectivity, and we have continued our work to find a more optimal ionic liquid for the separation of CO₂/H₂S.

In the present study, we measure for the first time the ternary phase behavior of CO₂/H₂S/[bmim][MeSO₄] and model the behavior using our cubic equation-of-state (EOS) method.^{14–17,32–34} The ternary EOS is based on the interaction parameters of each binary system. The VLE data for H₂S/[bmim][MeSO₄] were limited to a single isotherm due to a malfunction with the Hiden microbalance; therefore, VLLE measurements were also used to develop the EOS binary parameters. The interaction parameters for CO₂/H₂S and CO₂/[bmim][MeSO₄] were developed in our previous reports^{32,34} and from literature data.^{13,35}

To check the validity of the ternary EOS, VLE experiments for the CO₂/H₂S/[bmim][MeSO₄] system were performed under various *T*, *P*, and feed compositions, and the EOS validity was satisfactorily confirmed. Then, the CO₂/H₂S selectivity with and without RTIL [bmim][MeSO₄] was calculated at several feed, *T*, and *P* conditions. The selectivity advantage using this RTIL is discussed based on the present ternary phase calculations.

Experimental Section

Materials. Hydrogen sulfide (mole fraction purity > 0.995, CAS no. 7783-06-4) and carbon dioxide (mole fraction purity > 0.9999, CAS no. 124-38-9) were purchased from MG Industries (Philadelphia, Pennsylvania). Hydrogen sulfide is classified as an extremely hazardous gas, and caution must be used when handling. Hydrogen sulfide is flammable and highly toxic with an (8 to 12) h allowable exposure limit (AEL) of 10 ppm. In our experiment, the H₂S cylinder and samples were always handled and stored in a ventilated hood. Proper personal protective equipment was worn when preparing and handling samples, and all materials were disposed of by incineration. Hydrogen sulfide has a strong odor which is easily detectable (0.0047 ppm odor threshold); however, loss of sensitivity is known to occur after initial exposure, and proper handling precautions must be taken.³² The [bmim][MeSO₄] (C₉H₁₈N₂O₄S, lot number: 99/851, CAS no. 401788-98-5) was obtained from Solvent Innovations (now part of EMD Chemicals Inc., Gibbstown, New Jersey). Figure 1 provides the chemical structure. The [bmim][MeSO₄] ionic liquid sample was dried and degassed by first placing the sample in a borosilicate glass tube and pulling a vacuum on the sample with a diaphragm pump (model: MVPO55-3, Pfeiffer) for about 3 h. Next, the sample was fully evacuated using a turbopump (model: TSH-071, Pfeiffer) to a pressure of about 5 · 10⁻³ kPa while simultaneously heating and stirring the ionic liquid at a temperature of about 348 K for 2 days. The final water content was measured by Karl Fischer titration (Aqua-Star C3000, solutions AquaStar Coulomat C and A), and the ionic liquid contained approximately 600 · 10⁻⁶ of water (mass basis).

Binary VLE Measurements. In this work, we measured the gas solubility of H₂S in [bmim][MeSO₄] using a gravimetric microbalance (model: IGA 003, Hiden Isochema Ltd.). Detailed descriptions of the experimental equipment and procedures for

Table 1. Experimental VLE for H₂S (1) + [bmim][MeSO₄] (2)

<i>T</i> /K	<i>P</i> /MPa	100 <i>x</i> ₁
298.1	0.0108	2.2
298.1	0.0257	4.4
298.1	0.0507	7.7
298.1	0.0753	10.8
298.1	0.1002	13.8
298.1	0.2510	27.0
298.1	0.5008	42.4
298.1	0.7509	52.1

the VLE are given in our previous reports.^{17,36} Hiden was consulted prior to making the measurements but did not have any experience with the compatibility of H₂S and their balance. We decided to attempt the measurements even after considering the possibility that we could damage the balance due to the corrosivity of H₂S. To the best of our knowledge, we are the first to measure the solubility of H₂S in an ionic liquid using a Hiden gravimetric microbalance. A dryer trap was installed prior to the H₂S entering the microbalance to remove moisture that could accelerate corrosion. Our initial intent was to measure the gas solubility at four temperatures over a range in pressure from (0.01 to 1.75) MPa at (298, 323, and 348) K and from (0.01 to 1.25) MPa at 283 K. Initial experiments with an empty sample container were conducted successfully at each temperature over the given range in pressure to properly account for the buoyancy effects.^{17,36} The first isotherm with a sample of [bmim][MeSO₄] was measured at 298 K, and mass measurements were made at pressures up to 0.75 MPa [(0.01, 0.025, 0.05, 0.075, 0.1, 0.25, 0.50, and 0.75) MPa] as shown in Table 1. During the solubility measurement at 298 K and 1.0 MPa, the mass reading on the microbalance went off scale to a high value and no longer changed as the pressure was increased. The H₂S was evacuated from the system, and a representative from Hiden was contacted to dismantle the system. The failure was diagnosed by Hiden and caused by the interaction of H₂S with a copper coil inside the microbalance. H₂S is known to react with copper to form copper sulfide which is a dark solid. Visual evidence of copper sulfide was seen on the exterior of the copper coil as well as on the copper gasket between the reactor and balance. The balance was repaired, and we are working with Hiden to develop a new balance that will be compatible with corrosive gases such as H₂S.

Solubility data of CO₂ and [bmim][MeSO₄] were taken from Kumelan et al.,³⁵ and the CO₂/H₂S data were taken from Bierlein and Kay.¹³

Binary VLLE Measurements. Four high-pressure sample containers were filled with dried [bmim][MeSO₄] following the procedures outlined in our previous publications.^{37,38} Only the tube containing a mole fraction of 98.3 % H₂S showed two liquid phases at 298 K. The tube containing a mole fraction of 98.8 % H₂S was single phase at room temperature but split into two phases at temperatures above 306.6 K. The other two samples (mole fractions of 82.6 % and 99.6 % H₂S) remained single phase in the temperature range (298 to 318) K. This was the first indication that the LLE gap was highly unusual.

VLLE experiments have been made with these samples at constant temperatures from about (306 to 318) K using the volumetric method.^{37,38} The VLLE determined by this method required only mass and volume measurements without any analytical method for molar composition or chemical analysis. Special attention must be given to ensure no leaks occur from the sample containers after being filled with the high-pressure H₂S. Weights of sample containers were checked several times before starting and after completing the VLLE experiments to

Table 2. H₂S (1) + [bmim][MeSO₄] (2) System

T K			\bar{V}^{ra}	\bar{V}^a	$\bar{V}^{ex,b}$	\bar{V}^{exb}
	100 x'_1	100 x_1	cm ³ ·mol ⁻¹	cm ³ ·mol ⁻¹	cm ³ ·mol ⁻¹	cm ³ ·mol ⁻¹
306.6	97.7 ± 0.1	98.8 ± 0.1	45.6 ± 0.2	46.6 ± 0.1	-3.4 ± 0.2	-0.6 ± 0.1
307.0	97.6 ± 0.1	98.9 ± 0.1	44.9 ± 0.2	46.8 ± 0.1	-4.3 ± 0.2	-0.4 ± 0.1
307.8	97.4 ± 0.1	98.9 ± 0.1	46.0 ± 0.1	47.0 ± 0.1	-3.6 ± 0.1	-0.2 ± 0.1
313.0	96.8 ± 0.1	99.1 ± 0.1	45.8 ± 0.1	48.0 ± 0.1	-5.6 ± 0.1	0.3 ± 0.1
318.0	96.4 ± 0.1	99.2 ± 0.1	45.6 ± 0.4	49.1 ± 0.2	-7.3 ± 0.4	0.6 ± 0.2

^a Observed molar volume. ^b Excess molar volume.

quantify whether any H₂S had escaped from the sample container. The samples were placed inside a constant-temperature water bath and were mechanically mixed while immersed in the tank.³⁷ The bath temperature was calibrated using a standard platinum resistance thermometer (model: 5699, Hart Scientific, range (73 to 933) K) and Blackstack readout (model: 1560 with SPRT module 2560). The Blackstack instrument and SPRT are a certified secondary temperature standard with a NIST traceable accuracy to ± 0.005 K. The uncertainty in the bath temperature was 0.2 K.

One of the most useful aspects of the present VLE method is the ability to obtain the molar volume of each separated liquid simultaneously with the mole fraction of each liquid at any given isothermal condition. Then, the excess molar volume (or volume of mixing) of each liquid solution (V^E and V^E) can be obtained, by use of the pure component molar volumes V_1^0 (H₂S) and V_2^0 ([bmim][MeSO₄]) using

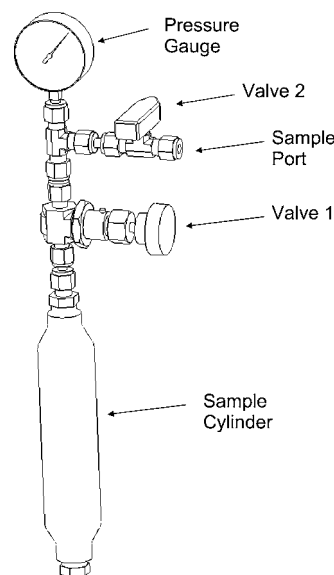
$$V^E = V_m - x'_1 V_1^0 - x'_2 V_2^0 \text{ or } V^E = V_m - x_1 V_1^0 - x_2 V_2^0 \quad (1)$$

where V_m is the measured molar volume of the mixture ($V_m = V'$ for the lower phase L' or $V_m = V$ for the upper phase L), and (x'_1, x'_2 or x_1, x_2) are mole fractions of H₂S (1) and [bmim]-[MeSO₄] (2) in phase L' and L, respectively. Saturated liquid molar volumes for H₂S were calculated using the NIST REFPROP EOS program.³⁹ The molar volume for [bmim]-[MeSO₄] was calculated from known liquid density data.⁴⁰

It is important to mention that the density of the vapor phase, which contains H₂S with a negligible contribution of [bmim]-[MeSO₄], must be properly accounted for in the mass balance equations. Observed liquid phase compositions and molar volumes for H₂S + [bmim][MeSO₄] are shown in Table 2, respectively. Total uncertainties ($\delta x_{TE} = (\delta x_{RE}^2 + \delta x_{SE}^2)^{1/2}$) were estimated by calculating both the overall random (δx_{RE}) and systematic errors (δx_{SE}). The following experimental parameters were considered to have an effect on the random errors: sample container calibration constants, mass of H₂S and [bmim]-[MeSO₄], height of lower and upper phases. The heights had the largest overall effect. The systematic errors include properly correcting for the sample level, area expansion, meniscus, and vapor phase moles. For additional details on estimation of total errors, see our previous work.^{37,38}

Ternary VLE Measurements. We have also conducted VLE experiments for the present ternary system (CO₂/H₂S/[bmim]-[MeSO₄]) at several thermodynamic conditions similar to our previous experiments with CO₂/H₂S/[bmim][PF₆]³² and CO₂/SO₂/[bmim][MeSO₄]³⁴ to verify the present EOS model.

Ten sample cells have been constructed as shown in Figure 2. Each cell was made using Swagelok fittings, two Swagelok valves (valve 1 is a stem valve, part number SS-4JB1, and valve 2 is a ball valve, part number SS-426S4), a stainless steel cylinder, and a pressure gauge (Parker Instruments, (0 to 0.7)

**Figure 2.** Schematic diagram of a sample cell.

MPa). The internal volume of each cell was estimated by measuring the mass of methanol required to completely fill one of the cells and knowing the density of methanol at the fill temperature. The internal volume of the cells (V_T) was (90 ± 2.5) cm³. Ionic liquid was loaded by mass [(0.88 to 10.06) g] inside a nitrogen-purged drybox. To load ionic liquid in the cell, the pressure gauge, valves, and fittings were removed, and a glass pipet (10 mL) which fit through the cylinder opening was used for filling. The pressure gauge, valves, and fittings were assembled as shown in Figure 2, and the sample cell was removed from the drybox. After filling with the ionic liquid, the sample cell was always maintained in a vertical upright position when valve 1 was open to prevent ionic liquid from coming in contact with the valves and pressure gauge. If the sample cell had to be mixed or weighed in a horizontal position, valve 1 would be closed and then reopened once the cylinder was in the vertical position again. The cell was connected to a diaphragm pump, with both valves open, to remove residual nitrogen. After the cell was evacuated, the ball valve (valve 2) was closed, and the cell was weighed on an analytical balance with a resolution of 0.01 g (model: PG-4002-S, Mettler Toledo) to obtain the initial ionic liquid mass.

The CO₂/H₂S gas mixtures were loaded by mass [(0.56 to 1.01) g] from a high-pressure gas cylinder. Three CO₂/H₂S gas mixtures (10.7/89.3, 58.2/41.8, and 96.9/3.1 mol ratios CO₂/H₂S) were prepared by weight and analyzed by gas chromatography (GC) (model: HP6890, Hewlett-Packard) using an isothermal (353.15 K) method (model: 113-4362, GS-GASPRO capillary column, 60 m length, 0.32 mm I.D., Agilent Technologies, inlet injector temperature 473.15 K, thermal conductivity detector temperature 523.15 K, helium carrier gas, flow rate 55 cm³·min⁻¹ with a 20:1 split ratio, injection volume 25 μ L). Special care must be taken when preparing the CO₂/H₂S gas mixtures to prevent condensation of H₂S. The saturation vapor pressure for CO₂ at 293 K is 6.0 MPa; however, the saturation pressure for H₂S at 293 K is lower at 1.78 MPa. Therefore, the total pressures for the three gas mixtures (10.7/89.3, 58.2/41.8, and 96.9/3.1 mol ratios CO₂/H₂S) were (1.07, 1.07, and 1.03) MPa, respectively.

The sample cells were set upright in a ventilated hood at room temperature for 48 h before any measurements were made. The sample cells were vigorously shaken periodically to assist with

mixing, and the pressure levels were monitored over time until they remained constant. The final weight and pressure of each cell was recorded. The process was repeated at a high temperature of about 315 K by placing the sample cells in a water bath (i.e., Plexiglas tank) and controlling the temperature with an external chiller (model: 1160S, VWR International), which circulated water through a copper coil inside the tank. The bath was stirred with an agitator (model: 1750, Arrow Engineering Co., Inc.) and the temperature measured with a thermocouple (model: 52II thermometer, Fluke). The sample cells were vigorously shaken to assist with mixing prior to being immersed in the tank. The water level in the tank was adjusted such that the entire cell was under water including both valves but not the pressure gauge. To ensure the samples were at equilibrium and properly mixed, the cells were momentarily removed from the water bath and vigorously shaken. The cells were placed back in the bath, and the process was repeated until no change in pressure was measured.

The pressure gauges were calibrated using the reference pressure transducer (model: 765-1K, Paroscientific). The Fluke thermometer was calibrated using the standard platinum resistance thermometer (model: 5699, Hart Scientific, range (73 to 933) K) and Blackstack readout (model: 1560 with SPRT module 2560). The temperature and pressure uncertainties were ± 0.2 K and ± 0.005 MPa.

After the cells had reached equilibrium at each temperature, the vapor space of each sample was analyzed by placing a rubber septum over the end of valve 2 (see Figure 2) and inserting a gastight syringe (model: 80930, Hamilton Company) to remove a small sample (25 μ L) which was analyzed by GC. The CO₂ and H₂S peaks appeared at about (3.5 and 5.0) min, respectively, with a total method run time of 6.0 min.

Thermodynamic Model

To study the phase behavior of a ternary system of CO₂/H₂S/[bmim][MeSO₄], we have developed thermodynamic models based on equations of state (EOS), which have been successfully applied for refrigerant/lubricant oil mixtures,³³ various hydrofluorocarbons, and CO₂ mixtures with ionic liquids,^{14–17,41} along with the ternary systems of CO₂/SO₂/[hmim][Tf₂N],⁴² CO₂/SO₂/[bmim][MeSO₄],³⁴ and CO₂/H₂S/[bmim][PF₆].³² It is based on a generic Redlich–Kwong (RK) type of cubic EOS

$$P = \frac{RT}{V-b} - \frac{a(T)}{V(V+b)} \quad (2)$$

$$a(T) = 0.427480 \frac{R^2 T_c^2}{P_c} \alpha(T) \quad (3)$$

$$b = 0.08664 \frac{RT_c}{P_c} \quad (4)$$

The temperature-dependent part of the a parameter in the EOS for pure compounds is modeled by the following empirical formula^{14–17,32–34,41,42}

$$\alpha(T) = \sum_{k=0}^{\leq 3} \beta_k (1/T_r - T_r^k), \quad (T_r \equiv T/T_c) \quad (5)$$

The coefficients, β_k , are determined to reproduce the vapor pressure of each pure compound.

The a and b parameters for general N -component mixtures are modeled in terms of their respective binary interaction parameters.^{14–17,32–34,41,42}

$$a = \sum_{ij=1}^N \sqrt{a_i a_j} f_{ij}(T) (1 - k_{ij}) x_i x_j, \quad a_i = 0.427480 \frac{R^2 T_{ci}^2}{P_{ci}} \alpha_i(T) \quad (6)$$

$$f_{ij}(T) = 1 + \tau_{ij}/T, \quad \text{where } \tau_{ij} = \tau_{ji}, \quad \text{and } \tau_{ii} = 0 \quad (7)$$

$$k_{ij} = \frac{l_{ij} l_{ji} (x_i + x_j)}{l_{jr} x_i + l_{ir} x_j}, \quad \text{where } k_{ii} = 0 \quad (8)$$

$$b = \frac{1}{2} \sum_{ij=1}^N (b_i + b_j) (1 - k_{ij}) (1 - m_{ij}) x_i x_j, \quad b_i = 0.08664 \frac{RT_{ci}}{P_{ci}} \quad (9)$$

where $m_{ij} = m_{ji}$, $m_{ii} = 0$; T_{ci} is critical temperature of the i th species; P_{ci} is critical pressure of the i -th species; R is universal gas constant; and x_i is mole fraction of the i th species. In the above model, there are a maximum of four binary interaction parameters, l_{ij} , l_{ji} , m_{ij} , and τ_{ij} , for each binary pair. However, only two or three parameters are sufficient for most cases. The fugacity coefficient ϕ_i of the i th species for the present EOS model, which is needed for the phase equilibrium calculation, is given by

$$\ln \phi_i = \ln \frac{RT}{P(V-b)} + b'_i \left(\frac{1}{V-b} - \frac{a}{RTb(V+b)} \right) + \frac{a}{RTb} \left(\frac{a'_i}{a} - \frac{b'_i}{b} + 1 \right) \ln \frac{V}{V+b} \quad (10)$$

where $a'_i \equiv [(\partial a)/(\partial n_i)]_{n_{j \neq i}}$ and $b'_i \equiv [(\partial b)/(\partial n_i)]_{n_{j \neq i}}$; n = total mole number; and n_i = mole number of the i th species (or $x_i = n_i/n$). The explicit forms of a'_i and b'_i may be useful for readers and are given as

$$a'_i = 2 \sum_{j=1}^N \sqrt{a_i a_j} f_{ij} x_j \left\{ 1 - k_{ij} - \frac{l_{ij} l_{ji} (l_{ij} - l_{ji}) x_i x_j}{(l_{jr} x_i + l_{ir} x_j)^2} \right\} - a \quad (11)$$

$$b'_i = \sum_{j=1}^N (b_i + b_j) (1 - m_{ij}) x_j \times \left\{ 1 - k_{ij} - \frac{l_{ij} l_{ji} (l_{ij} - l_{ji}) x_i x_j}{(l_{jr} x_i + l_{ir} x_j)^2} \right\} - b \quad (12)$$

The equilibrium solubility for the ternary VLE system can be obtained by solving the following equilibrium conditions

$$x_i \phi_i^L = y_i \phi_i^V \quad (i = 1, 2, 3) \quad (13)$$

Table 3. EOS Constants for Pure Compounds Used in the Present Study

	hydrogen sulfide ^a	carbon dioxide ^b	[bmim][MeSO ₄] ^c
molar mass/g·mol ⁻¹	34.08	44.01	250.32
<i>T_c</i> /K	373.60	304.13	920.1
<i>P_c</i> /MPa	9.0080	7.377	2.806
β_0	0.99879	1.00049	1.0
β_1	0.33206	0.43866	0.611705
β_2	-0.049417	-0.10498	---
β_3	0.0046387	0.06250	---

^a Taken from our previous work.³⁹ ^b Taken from our previous work.⁴⁴

^c Taken from our previous work.⁴⁵

Table 4. Optimal Binary Interaction Parameters in Equations 7 to 9

system (1)/(2)	<i>l</i> ₁₂	<i>l</i> ₂₁	<i>m</i> ₁₂ = <i>m</i> ₂₁	τ_{12} = τ_{21} /K
CO ₂ /H ₂ S ^a	0.04014	2.7134	0.0	-23.37
CO ₂ /[bmim][MeSO ₄] ^b	0.14237	0.16742	-0.18814	33.925
H ₂ S/[bmim][MeSO ₄]	0.1096932	0.0023	0.03659	1.5

^a Taken from our previous work.³² ^b Taken from our previous work.³⁴

where *x_i* is liquid mole fraction of the *i*th species (*x*₁ + *x*₂ + *x*₃ = 1); *y_i* is vapor mole fraction of the *i*th species (*y*₁ + *y*₂ + *y*₃ = 1); ϕ_i^L is liquid-phase fugacity coefficient of the *i*th species; and ϕ_i^V is vapor-phase fugacity coefficient of the *i*th species.

In the case of three-phase equilibria (VLLE), equations corresponding to eq 13 become

$$x_i^{L1} \phi_i^{L1} = x_i^{L2} \phi_i^{L2} = y_i^V \phi_i^V \quad (i = 1, \dots, N) \quad (14)$$

where superscripts L1 and L2 denote one liquid phase (1) and another coexisting liquid phase (2) of VLLE, respectively. Numerical solutions of eqs 13 or 14 (nonlinearly coupled equations) can be obtained by use of the *TP-Flash* (Rachford–Rice) method.⁴³

EOS Model Parameters. Pure component EOS parameters for hydrogen sulfide and carbon dioxide were determined based on data from the NIST REFPROP EOS database³⁹ and the literature,⁴⁴ respectively. For the ionic liquid, the critical parameters (*T_c* and *P_c*) and β_k in eqs 3 to 5 were taken from our previous work.⁴⁵ Table 3 shows the EOS constants for the present compounds. Binary interaction parameters, *l_{ij}*, *l_{ji}*, *m_{ij}*, and τ_{ij} , in eqs 7 to 9, for each binary pair were obtained using nonlinear regression analyses of experimental *PTx* (pressure–temperature–composition) data for CO₂ + [bmim][MeSO₄]³⁵ and CO₂ + H₂S¹³ systems. As mentioned earlier, the limited number of VLE data (single isotherm at 298.1 K from (0.01 to 0.75) MPa) for H₂S + [bmim][MeSO₄] required using some of the VLLE data [(307.8 and 313) K in Table 2] to develop the binary interaction parameters. The ([bmim][MeSO₄]-rich side) boundary was used to build the EOS model as well as the limited VLE (only up to about 52 mol %). Table 4 presents optimal binary interaction parameters for the present system pairs.

Figure 3a is a *PTx* phase diagram which shows our model predictions of H₂S solubilities in [bmim][MeSO₄] with the present VLE data. The standard deviation for the *P* versus *x*₁ fit is excellent (*dP* = 0.0073 MPa). EOS model predictions have also been compared with the observed VLLE data in Figure 3a and are in excellent agreement with the experimental data shown in Table 2. The VLLE for H₂S/[bmim][MeSO₄] is highly asymmetric with an unusually narrow (mole fraction H₂S between 0.97 and 0.99) LLE gap which to the best of our knowledge is the first such case reported in the literature. The present EOS was able to model this extremely narrow (only 2 mol %) and rare LLE gap successfully. The VLLE behavior suggests that

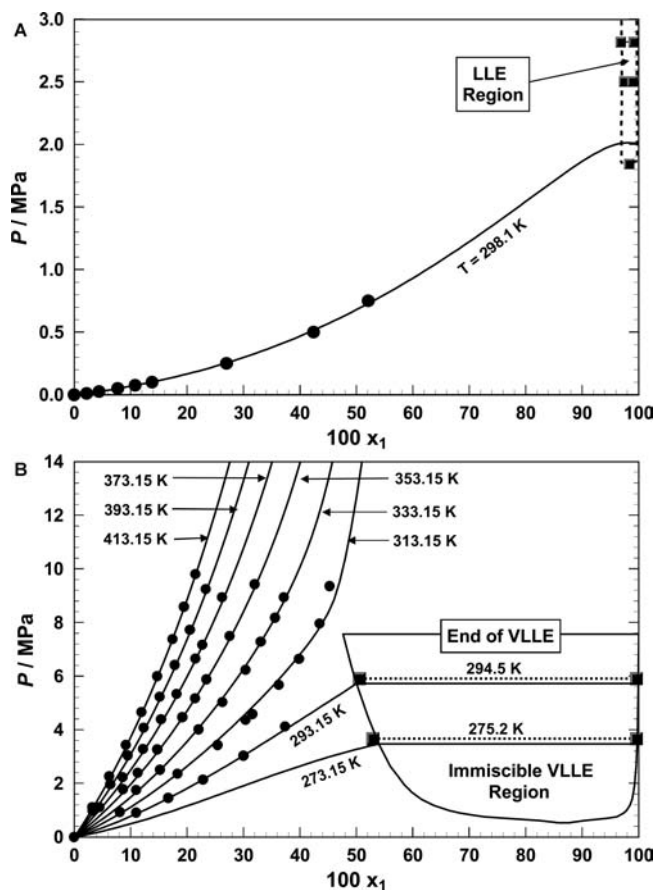


Figure 3. Isothermal *Px* (pressure–liquid composition) phase diagram. (a) *Px* phase diagram of the H₂S (1) + [bmim][MeSO₄] (2) binary system, lines: predicted by the present EOS calculations, symbols: ●, present VLE data; ■, present VLLE data. (b) *Px* phase diagram of the CO₂ (1) + [bmim][MeSO₄] (2) binary system, lines: EOS calculations;³⁴ symbols: ●, VLE data;³⁵ ■, VLLE data.³⁴

this binary system is Type V phase behavior, according to the classification of von Konynenburg and Scott.⁴⁶

Figure 3b is a similar plot of our model predictions of CO₂ VLE in [bmim][MeSO₄] using Kumelan et al.'s experimental data.³⁵ The standard deviation for the *P* versus *x*₁ fit is good (*dP* = 0.089 MPa). The present EOS has also predicted the VLLE (or liquid–liquid separation) in the CO₂-rich side solution, as shown in Figure 3b. This prediction has been well confirmed by the previous VLLE experiment.³⁴

Vapor–liquid equilibrium (VLE) data of CO₂ + H₂S mixtures obtained in the literature¹³ are shown in Figures 4a and 4b for selected isotherms [(303.15 and 333.15) K], compared with the present EOS calculations. It should be noted that no VLE exists at 333.15 K above mole fractions of about 50 % CO₂ in H₂S. Although the solubility behavior of each binary system has been well correlated with the present EOS model as illustrated in Figures 3 and 4, the phase behavior prediction of the *ternary system* of CO₂/H₂S/[bmim][MeSO₄] may not always be guaranteed based on the binary interaction parameters alone. Particularly for systems containing supercritical fluids and/or nonvolatile compounds such as the present case, the validity of a proposed EOS model for ternary mixtures must be checked experimentally.

Figure 5 presents the comparison of observed and calculated values for H₂S mole fraction in the vapor phase (CO₂ mole fraction = 1 – H₂S mole fraction, and [bmim][MeSO₄] mole fraction = 0) under various *T*, *P*, and feed composition

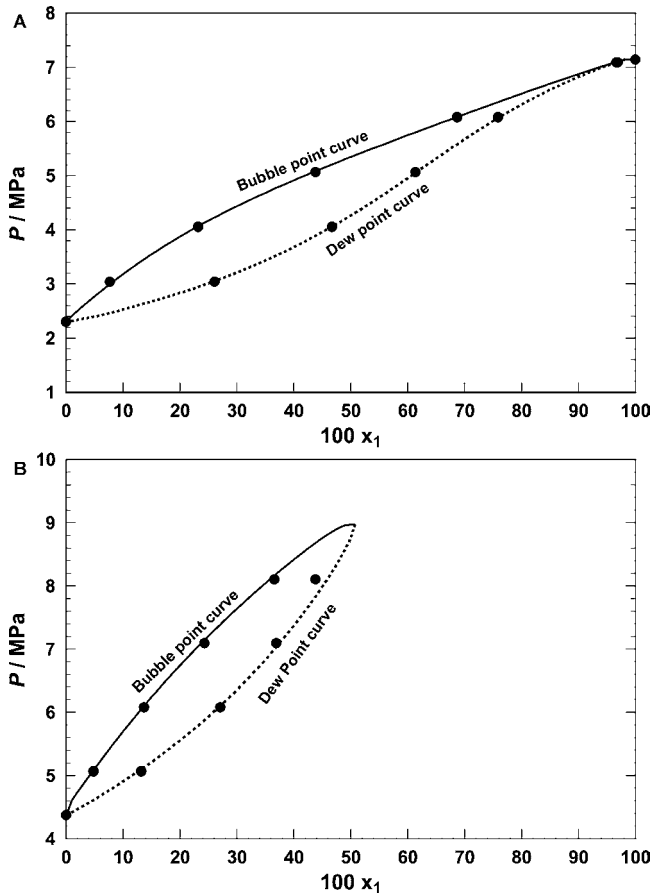


Figure 4. Isothermal VLE P_{xy} (pressure–liquid–vapor composition) diagrams of the binary CO_2 (1)/ H_2S (2) system. Lines: the present EOS calculations; solid lines, bubble point curves; broken lines, dew point curves. Symbols: experimental data¹³ (a) $T = 303.15$ K and (b) $T = 333.15$ K.

conditions (see Table 5). The calculated and measured H_2S vapor mole fraction data are in excellent agreement (< 0.01).

Results and Discussion

Since the present EOS model has been verified, we can predict the solubility behavior of the present ternary system with

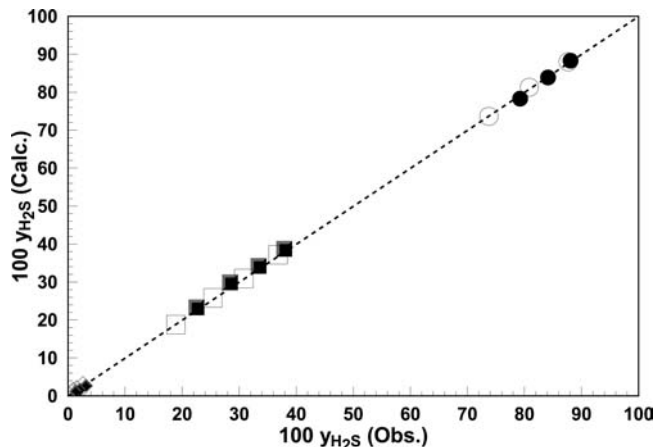


Figure 5. Comparison of experimental and calculated VLE data for the ternary $\text{CO}_2/\text{H}_2\text{S}/[\text{bmim}][\text{MeSO}_4]$ system. Calculated vapor-phase compositions of H_2S (CO_2 mole fraction = $1 - \text{H}_2\text{S}$ mole fraction) are compared with observed H_2S vapor compositions for various experimental conditions (see Table 5). Symbols: open symbols, about 296 K; solid symbols, about (314 to 315) K; circle symbols, 10.7/89.3 mol ratio $\text{CO}_2/\text{H}_2\text{S}$ feed; square symbols, 58.2/41.8 mol ratio $\text{CO}_2/\text{H}_2\text{S}$ feed; diamond symbols, 96.9/3.1 mol ratio $\text{CO}_2/\text{H}_2\text{S}$ feed.

confidence. To assess the feasibility of the gas separation by the extractive distillation or selective absorption method, gaseous selectivity $\alpha_{A/B}$, ability to separate gases A and B in the gas phase, or gaseous absorption, selectivity $S_{B/A}$ in the liquid phase is commonly defined as^{47–49}

$$\alpha_{A/B} = S_{B/A} = \left(\frac{y_A}{x_A} \right) / \left(\frac{y_B}{x_B} \right) \quad (15)$$

where x_A (or x_B) and y_A (or y_B) are the mole fractions of A (or B) in the ionic liquid solution phase and vapor phase, respectively. Here we denote CO_2 as A and H_2S as B. The $\text{CO}_2/\text{H}_2\text{S}$ selectivity ($\alpha_{A/B}$) in the gas phase has been examined using the present EOS model at various T , P , and feed compositions, and results are shown in Figures 6, 7, and 8.

Table 5. Experimental VLE Data for Ternary Mixtures of CO_2 (1) + H_2S (2) + $[\text{bmim}][\text{MeSO}_4]$ (3)^a

feed	feed	feed	T	P	calculated	calculated	calculated	measured
100 x_1	100 x_2	100 x_3	K	MPa	100 x_2	100 x_3	100 y_2	100 y_2
84.1 ± 0.5	2.7 ± 0.1	13.2 ± 0.5	295.8	0.7219	3.2 ± 0.2	88.6 ± 0.2	2.6 ± 0.2	2.6 ± 1.0 ^a
41.4 ± 0.9	1.3 ± 0.1	57.3 ± 0.9	296.4	0.4530	1.2 ± 0.2	93.2 ± 0.2	1.5 ± 0.2	1.5 ± 1.0 ^a
25.2 ± 0.7	0.8 ± 0.1	74.0 ± 0.7	295.8	0.4244	0.8 ± 0.2	93.8 ± 0.2	1.0 ± 0.2	0.9 ± 0.9 ^a
45.4 ± 0.5	32.6 ± 0.4	22.0 ± 0.9	296.7	0.4461	21.5 ± 0.3	75.5 ± 0.3	37.2 ± 0.5	36.8 ± 1.0 ^b
32.1 ± 0.6	23.1 ± 0.4	44.8 ± 1.0	296.2	0.3840	16.9 ± 0.3	80.1 ± 0.4	30.9 ± 0.7	30.8 ± 1.0 ^b
25.3 ± 0.5	18.2 ± 0.7	56.7 ± 0.9	296.4	0.3909	14.8 ± 0.6	82.0 ± 0.5	25.8 ± 1.2	25.4 ± 1.0 ^b
17.0 ± 0.4	12.2 ± 0.3	70.8 ± 0.7	296.1	0.3633	10.8 ± 0.3	85.7 ± 0.3	18.8 ± 0.6	18.9 ± 1.0 ^b
8.6 ± 0.1	72.1 ± 0.8	19.2 ± 0.9	296.3	0.4392	38.2 ± 0.4	60.6 ± 0.4	88.0 ± 0.4	87.7 ± 1.0 ^c
4.9 ± 0.1	40.7 ± 0.9	54.4 ± 1.0	296.0	0.3013	28.9 ± 0.4	70.2 ± 0.4	81.3 ± 1.1	80.9 ± 1.0 ^c
3.2 ± 0.1	26.7 ± 0.7	70.1 ± 0.8	296.4	0.2254	21.9 ± 0.6	77.2 ± 0.5	73.6 ± 1.9	73.8 ± 1.0 ^c
84.1 ± 0.5	2.7 ± 0.1	13.2 ± 0.5	315.3	0.7632	2.2 ± 0.2	91.4 ± 0.2	2.8 ± 0.2	3.1 ± 1.0 ^a
41.4 ± 0.9	1.3 ± 0.1	57.3 ± 0.9	315.3	0.4874	1.0 ± 0.2	94.6 ± 0.2	1.8 ± 0.2	2.0 ± 1.0 ^a
25.2 ± 0.7	0.8 ± 0.1	74.0 ± 0.7	315.3	0.4461	0.6 ± 0.2	95.3 ± 0.2	1.3 ± 0.2	1.3 ± 1.0 ^a
45.4 ± 0.5	32.6 ± 0.4	22.0 ± 0.9	315.3	0.4599	15.7 ± 0.2	82.0 ± 0.9	38.8 ± 0.5	37.9 ± 1.0 ^b
32.1 ± 0.6	23.1 ± 0.4	44.8 ± 1.0	315.1	0.4185	13.2 ± 0.3	84.5 ± 0.4	34.3 ± 0.8	33.4 ± 1.0 ^b
25.3 ± 0.5	18.2 ± 0.7	56.7 ± 0.9	314.5	0.4323	12.2 ± 0.5	85.2 ± 0.4	29.9 ± 1.3	28.4 ± 1.0 ^b
17.0 ± 0.4	12.2 ± 0.3	70.8 ± 0.7	314.2	0.4116	9.5 ± 0.3	87.7 ± 0.2	23.3 ± 0.8	22.5 ± 1.0 ^b
8.6 ± 0.1	72.1 ± 0.8	19.2 ± 0.9	314.5	0.4874	30.6 ± 0.2	68.6 ± 0.3	88.3 ± 0.3	88.1 ± 1.0 ^c
4.9 ± 0.1	40.7 ± 0.9	54.4 ± 1.0	314.4	0.3702	24.5 ± 0.4	74.8 ± 0.4	83.9 ± 0.8	84.2 ± 1.0 ^c
3.2 ± 0.1	26.7 ± 0.7	70.1 ± 0.8	314.4	0.2944	19.7 ± 0.4	79.6 ± 0.4	78.3 ± 1.5	79.3 ± 1.0 ^c

^a $\text{CO}_2/\text{H}_2\text{S}$ gas mixtures: a, (96.9/3.1) mole ratio; b, (58.2/41.8) mole ratio; c, (10.7/89.3) mole ratio). Liquid CO_2 mole fraction = ($x_1 = 1 - x_2 - x_3$). Vapor CO_2 mole fraction = ($y_1 = 1 - y_2$) and vapor $[\text{bmim}][\text{PF}_6]$ mole fraction = 0.

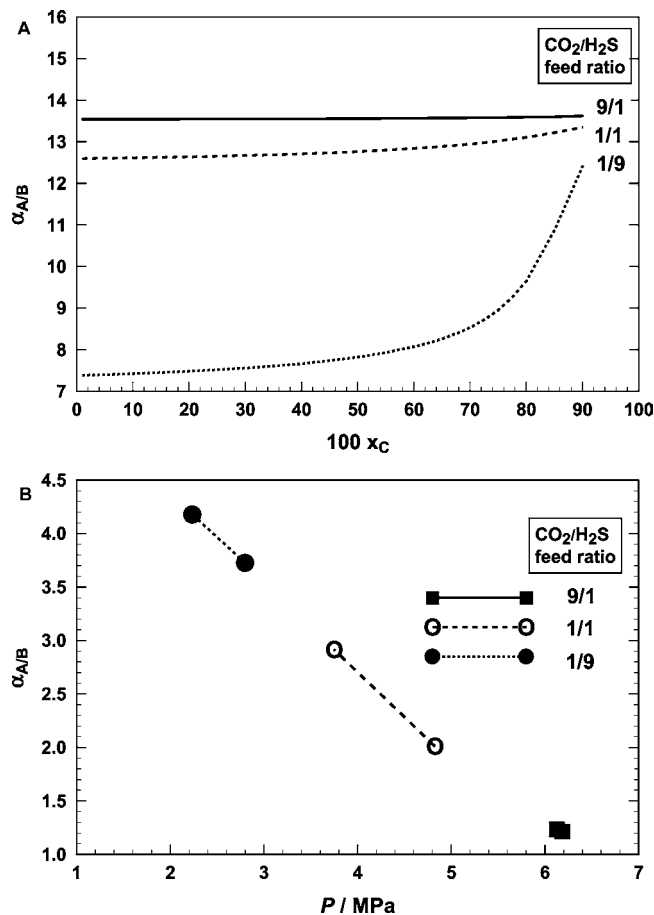


Figure 6. (a) Plots of calculated CO₂ (A)/H₂S (B) selectivity defined by eq 15 versus overall [bmim][MeSO₄] (C) mole fraction with three different CO₂/H₂S feed ratios (9/1, 1/1, and 1/9) at $T = 298.15$ K and $P = 0.1$ MPa. (b) Selectivity plots without ionic liquid [bmim][MeSO₄] as a function of total pressure. Three cases with different CO₂/H₂S feed ratios are shown at $T = 298.15$ K. Lines: solid line, 9/1 CO₂/H₂S feed mole ratio; broken line, 1/1 CO₂/H₂S feed mole ratio; dotted line, 1/9 CO₂/H₂S feed mole ratio.

In Figure 6a, the CO₂/H₂S selectivity ($\alpha_{A/B}$) is plotted as a function of the ionic liquid [bmim][MeSO₄] concentration for ternary mixtures with three CO₂/H₂S mole ratios (9/1, 1/1, and 1/9) at $T = 298.15$ K and $P = 0.1$ MPa. For mole ratios (9/1 and 1/1), the selectivity ($\alpha_{A/B}$) remains relatively constant at about 12.5 to 13.5 with increasing ionic liquid concentration. For a low mole ratio (1/9), the selectivity starts low (about 7.5) for low concentrations of IL. After the ionic liquid concentration increases above a mole fraction of 60 %, however, the selectivity begins to sharply increase to about 12.5.

To understand the change in selectivity due to the ionic liquid addition, Figure 6b provides clear insights, showing the selectivity *without* [bmim][MeSO₄] at 298.15 K as a function of pressure for the same CO₂/H₂S feed ratios (9/1, 1/1, and 1/9). The selectivity enhancement due to the ionic liquid addition can be well observed from the comparison between Figures 6a and 6b. For example, the feed ratio of 9/1 (CO₂/H₂S) with the ionic liquid has a selectivity of about 13.5, while the corresponding case *without* the ionic liquid shows a selectivity of about 1.2. As the feed ratio decreases (9/1 to 1/1 to 1/9 CO₂/H₂S), the improvement in selectivity with the ionic liquid versus without the ionic liquid also decreases but remains substantial.

The selectivity characteristics at a higher temperature (313.15 K) and pressures [(0.1 and 1) MPa] are shown in Figure 7, with and without the ionic liquid addition. The general behavior as shown in Figure 7 is similar to the case in Figure 6; however,

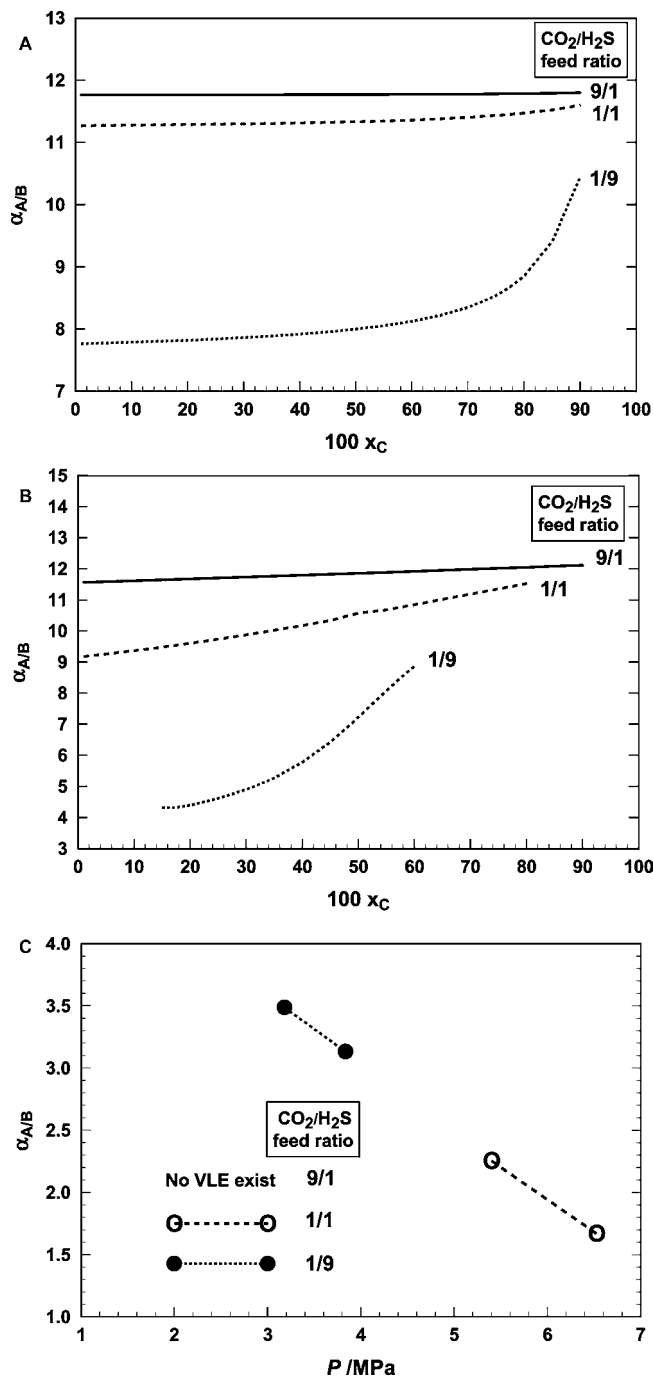


Figure 7. Plots of calculated CO₂ (A)/H₂S (B) selectivity defined by eq 15 versus overall [bmim][MeSO₄] (C) mole fraction with three different CO₂/H₂S feed ratios (9/1, 1/1, and 1/9) at (a) $T = 313.15$ K and $P = 0.1$ MPa and (b) $T = 313.15$ K and $P = 1$ MPa. (c) Selectivity plots without ionic liquid [bmim][MeSO₄] as a function of total pressure. Three cases with different CO₂/H₂S feed ratios are shown at $T = 313.15$ K. Lines: solid line, 9/1 CO₂/H₂S feed mole ratio; broken line, 1/1 CO₂/H₂S feed mole ratio; dotted line, 1/9 CO₂/H₂S feed mole ratio.

the selectivity enhancement with the ionic liquid addition is slightly lower. The most important fact to consider at higher temperature is that for high CO₂/H₂S feed ratios (9/1) no VLE exists without the ionic liquid, and the gas mixtures cannot be separated using traditional distillation methods as shown in Figure 7c. Therefore, only with the addition of the ionic liquid as shown in Figures 7a and 7b is separation of CO₂ and H₂S from high CO₂ content mixtures possible.

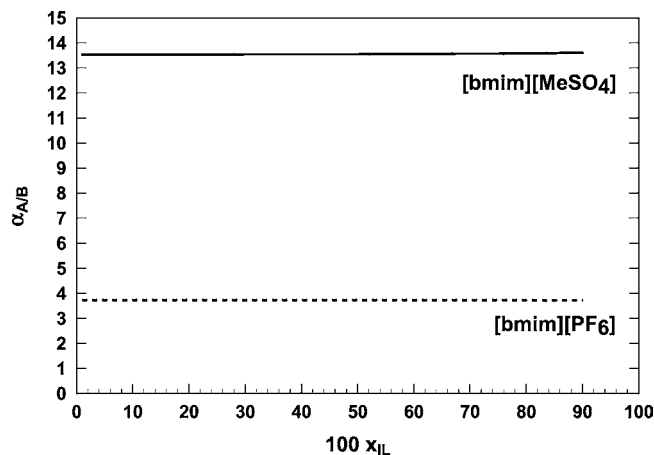


Figure 8. Comparison of calculated CO₂ (A)/H₂S (B) selectivity in [bmim][MeSO₄] versus [bmim][PF₆] at 9/1 CO₂/H₂S feed ratio, $T = 298.15$ K, and $P = 0.1$ MPa as a function of mole fraction ionic liquid (IL); [bmim][PF₆] data taken from previous work.³²

Figure 8 shows the remarkable increase in CO₂/H₂S selectivity for the feed ratio of 9/1 (CO₂/H₂S) using ionic liquid [bmim][MeSO₄] versus our previous report³² using [bmim][PF₆]. The increase in CO₂/H₂S selectivity (from 3.7 to 13.5) is due primarily to the strong chemical absorption for H₂S in [bmim][MeSO₄] versus H₂S in [bmim][PF₆].

Finally, it should be mentioned that negative excess molar volumes in [bmim][MeSO₄]-rich side solutions have been observed for both the CO₂ and H₂S binary systems. In the case of the CO₂ + [bmim][MeSO₄] and H₂S + [bmim][MeSO₄] binary systems, the ionic liquid rich side solution molar volumes are largely negative (e.g. $(-5$ to $-9)$ cm³·mol⁻¹) and (e.g. $(-3$ to $-7)$ cm³·mol⁻¹), respectively. These values are similar to our previous studies of other binary systems containing CO₂ + ionic liquids (e.g. [hmim][Tf₂N]¹⁴ and [bmim][acetate]¹⁵) and hydrofluorocarbons (HFCs) + ionic liquids.^{37,38,41} This clearly indicates that RTILs with gases such as CO₂, H₂S, and HFCs have quite large negative excess molar volumes compared with what have been reported with ordinary liquid mixtures (typically about $(0$ to $\pm 3)$ cm³·mol⁻¹).⁵⁰ Explaining this phenomenon poses a unique and interesting challenge for theoretical modelers. One possible explanation by Huang et al.⁵¹ for the CO₂ + [bmim][PF₆] system indicates that small angular rearrangements of the anion are occurring which create localized cavities that allow CO₂ to fit above and below the imidazolium ring without much change from the molar volume of pure IL. Similar rearrangements may be occurring with H₂S and CO₂ in other RTILs, and additional forces, such as hydrogen bonding, may also be involved.

Conclusions

Although the separation concept of gaseous mixtures using room-temperature ionic liquids has been proposed in the past, demonstrations for CO₂/H₂S reported in the literature are limited. In this report, we have developed for the first time a reliable EOS model for the ternary CO₂/H₂S/[bmim][MeSO₄] system and have examined the gaseous selectivity of these acid gases, using ionic liquid [bmim][MeSO₄]. The corrosive nature of H₂S attacked the copper materials inside the microbalance which led to a malfunction; however, a limited number of VLE data were collected and combined with some of the VLLE data for H₂S/[bmim][MeSO₄] to construct the binary EOS model parameters. The VLLE for H₂S/[bmim][MeSO₄] is highly asymmetric with an unusually

narrow (mole fraction H₂S between 0.97 and 0.99) LLE gap which to the best of our knowledge is the first such case reported in the literature. The present EOS was able to model this extremely narrow (2 mol %) and rare LLE gap successfully. The ternary VLE data were extremely useful and sensitive to the binary H₂S/[bmim][MeSO₄] EOS construction and validated our results.

The choice of [bmim][MeSO₄] led to a significant increase in the CO₂/H₂S selectivity compared with our previous work using [bmim][PF₆]. The increase in CO₂/H₂S selectivity (from 3.7 to 13.5) for a CO₂/H₂S feed ratio of 9/1 is due primarily to the strong chemical absorption behavior for H₂S in [bmim][MeSO₄] versus H₂S in [bmim][PF₆]. The present ionic liquid ([bmim][MeSO₄]) may still not be the best choice for the gaseous separation and/or capturing of CO₂ and H₂S; however, it does prove that the choice of the ionic liquid can lead to a significant improvement in the gaseous selectivity.

Acknowledgment

The authors thank Mr. Brian L. Wells for his assistance with the vapor–liquid equilibrium measurements.

Literature Cited

- Speyer, D.; Ermatchkov, V.; Maurer, G. Solubility of carbon dioxide in aqueous solutions of N-methyldiethanolamine and piperazine in the low gas loading region. *J. Chem. Eng. Data* **2010**, *55*, 283–290.
- Böttger, A.; Ermatchkov, V.; Maurer, G. Solubility of carbon dioxide in aqueous solutions of N-methyldiethanolamine and piperazine in the high gas loading region. *J. Chem. Eng. Data* **2009**, *54*, 1905–1909.
- Mandal, B. P.; Biswas, A. K.; Bandyopadhyay, S. S. Selective absorption of H₂S from gas streams containing H₂S and CO₂ into aqueous solutions of N-methyldiethanolamine and 2-amino-2-methyl-1-propanol. *Sep. Purif. Technol.* **2004**, *35*, 191–202.
- Mandal, B. P.; Bandyopadhyay, S. S. Simultaneous absorption of carbon dioxide and hydrogen sulfide into aqueous blends of 2-amino-2-methyl-1-propanol and diethanolamine. *Chem. Eng. Sci.* **2005**, *60*, 6438–6451.
- Lee, J. I.; Otto, F. D.; Mather, A. E. Solubility of mixtures of carbon dioxide and hydrogen sulfide in 5.0N monoethanolamine solution. *J. Chem. Eng. Data* **1975**, *20*, 161–163.
- Jane, I.-S.; Li, M.-H. Solubilities of mixtures of carbon dioxide and hydrogen sulfide in water + diethanolamine + 2-amino-2-methyl-1-propanol. *J. Chem. Eng. Data* **1997**, *42*, 98–105.
- Deshmukh, R. D.; Mather, A. E. A mathematical model for equilibrium solubility of hydrogen sulfide and carbon dioxide in aqueous alkanolamine solutions. *Chem. Eng. Sci.* **1981**, *36*, 355–362.
- Kuranov, G.; Rumpf, B.; Smirnova, N. A.; Maurer, G. Solubility of single gases carbon dioxide and hydrogen sulfide in aqueous solutions of N-methyldiethanolamine in the temperature range 313–413 K at pressures up to 5 MPa. *Ind. Eng. Chem. Res.* **1996**, *35*, 1959–1966.
- Pérez-Salado Kamps, Á.; Balaban, A.; Jödecke, M.; Kuranov, G.; Smirnova, N. A.; Maurer, G. Solubility of single gases carbon dioxide and hydrogen sulfide in aqueous solutions of N-methyldiethanolamine at temperatures from 313 to 393 K and pressures up to 7.6 MPa: New experimental data and model extension. *Ind. Eng. Chem. Res.* **2001**, *40*, 696–706.
- Finotello, A.; Bara, J. E.; Camper, D.; Noble, R. D. Room-temperature ionic liquids: Temperature dependence of gas solubility selectivity. *Ind. Eng. Chem. Res.* **2008**, *47*, 3453–3459.
- Mayland, B. J. Removal of Carbon Dioxide and Hydrogen Sulfide from Gaseous Mixtures. U.S. Patent 3,275,403, 1966.
- Benson, H. E. Separation of Carbon Dioxide and Hydrogen Sulfide from Gas Mixtures. U.S. Patent 3,642,430, 1972.
- Bierlein, J. A.; Kay, W. B. Phase-Equilibrium Properties of System Carbon Dioxide-Hydrogen Sulfide. *Ind. Eng. Chem.* **1952**, *45*, 618–624.
- Shiflett, M. B.; Yokozeki, A. Solubility of CO₂ in room temperature ionic liquid [hmim][Tf₂N]. *J. Phys. Chem. B* **2007**, *111*, 2070–2074.
- Shiflett, M. B.; Kasprzak, D. J.; Junk, C. P.; Yokozeki, A. Phase behavior of {carbon dioxide + [bmim][Ac]} mixtures. *J. Chem. Thermodyn.* **2008**, *40*, 25–31.
- Yokozeki, A.; Shiflett, M. B.; Junk, C. P.; Grieco, L. M.; Foo, T. Physical and chemical absorptions of carbon dioxide in room-temperature ionic liquids. *J. Phys. Chem. B* **2008**, *112*, 16654–16663.

- (17) Shiflett, M. B.; Yokozeki, A. Solubilities and Diffusivities of Carbon Dioxide in Ionic Liquids: [bmim][PF₆] and [bmim][BF₄]. *Ind. Eng. Chem. Res.* **2005**, *44*, 4453–4464.
- (18) Pérez-Salado Kamps, Á.; Tuma, D.; Xia, J.; Maurer, G. Solubility of CO₂ in the ionic liquid [bmim][PF₆]. *J. Chem. Eng. Data* **2003**, *48*, 746–749.
- (19) Husson-Borg, P.; Majer, V.; Costa Gomes, M. F. Solubilities of oxygen and carbon dioxide in butyl methyl imidazolium tetrafluoroborate as a function of temperature and at pressures close to atmospheric pressure. *J. Chem. Eng. Data* **2003**, *48*, 480–485.
- (20) Shariati, A.; Peters, C. J. High-pressure phase behavior of systems with ionic liquids: Part III. The binary system carbon dioxide + 1-hexyl-3-methylimidazolium hexafluorophosphate. *J. Supercrit. Fluids* **2004**, *30*, 139–144.
- (21) Shariati, A.; Gutkowski, K.; Peters, C. J. Comparison of the phase behavior of some selected binary systems with ionic liquids. *AIChE J.* **2005**, *51*, 1532–1540.
- (22) Scovazzo, P.; Camper, D.; Hieft, J.; Poshusta, J.; Koval, C.; Noble, R. Regular solution theory and CO₂ gas solubility in room-temperature ionic liquids. *Ind. Eng. Chem. Res.* **2004**, *43*, 6855–6860.
- (23) Liu, Z.; Wu, W.; Han, B.; Dong, Z.; Zhao, G.; Wang, J.; Jiang, T.; Yang, G. Study on the phase behaviors, viscosities, and thermodynamic properties of CO₂/[C₄mim][PF₆]/methanol system at elevated pressures. *Chem.—Eur. J.* **2003**, *9*, 3897–3903.
- (24) Aki, S. N. V. K.; Mellein, B. R.; Saurer, E. M.; Brennecke, J. F. High-pressure phase behavior of carbon dioxide with imidazolium-based ionic liquids. *J. Phys. Chem. B* **2004**, *108*, 20355–20365.
- (25) Blanchard, L. A.; Gu, G.; Brennecke, J. F. High-pressure phase behavior of ionic liquid/CO₂ systems. *J. Phys. Chem. B* **2001**, *105*, 2437–2444.
- (26) Shiflett, M. B.; Yokozeki, A. Phase behavior of carbon dioxide in ionic liquids: [emim][acetate], [emim][trifluoroacetate], and [emim][acetate] + [emim][trifluoroacetate] mixtures. *J. Chem. Eng. Data* **2009**, *54*, 108–114.
- (27) Carvalho, P. J.; Álvarez, V. H.; Schröder, B.; Gil, A. M.; Marrucho, I. M.; Aznar, M.; Santos, L. M. N. B. F.; Coutinho, J. A. P. Specific solvation interactions of CO₂ on acetate and trifluoroacetate imidazolium based ionic liquids at high pressures. *J. Phys. Chem. B* **2009**, *113*, 6803–6812.
- (28) Jou, F.-Y.; Mather, A. E. Solubility of hydrogen sulfide in [bmim][PF₆]. *Int. J. Thermophys.* **2007**, *28*, 490–495.
- (29) Pomelli, C. S.; Chiappe, C.; Vidis, A.; Laurenczy, G.; Dyson, P. J. Influence of the interactions between hydrogen sulfide and ionic liquids on solubility: Experimental and theoretical investigation. *J. Phys. Chem. B* **2007**, *111*, 13014–13019.
- (30) Heintz, Y. J.; Sehabiague, L.; Morsi, B. I.; Jones, K. L.; Luebke, D. R.; Pennline, H. W. Hydrogen sulfide and carbon dioxide removal from dry fuel gas streams using an ionic liquid as a physical solvent. *Energy Fuel* **2009**, *23*, 4822–4830.
- (31) Jalili, A. H.; Rahmati-Rostami, M.; Ghotbi, C.; Hosseini-Jenab, M.; Ahmadi, A. N. Solubility of H₂S in ionic liquids [bmim][PF₆], [bmim][BF₄], and [bmim][Tf₂N]. *J. Chem. Eng. Data* **2009**, *54*, 1844–1849.
- (32) Shiflett, M. B.; Yokozeki, A. Separation of CO₂ and H₂S using room-temperature ionic liquid [bmim][PF₆]. *Fluid Phase Equilib.* **2010**, *294*, 105–113.
- (33) Yokozeki, A. Solubility of refrigerants in various lubricants. *Int. J. Thermophys.* **2001**, *22*, 1057–1071.
- (34) Shiflett, M. B.; Yokozeki, A. Separation of Carbon Dioxide and Sulfur Dioxide Using Room-Temperature Ionic Liquid [bmim][MeSO₄]. *Energy Fuel* **2010**, *24*, 1001–1008.
- (35) Kumelan, J.; Pérez-Salado Kamps, Á.; Tuma, D.; Maurer, G. Solubility of CO₂ in the ionic liquids [bmim][CH₃SO₄] and [bmim][PF₆]. *J. Chem. Eng. Data* **2006**, *51*, 1802–1807.
- (36) Shiflett, M. B.; Yokozeki, A. Solubility and diffusivity of hydrofluorocarbons in room-temperature ionic liquids. *AIChE J.* **2006**, *52*, 1205–1219.
- (37) Shiflett, M. B.; Yokozeki, A. Vapor-liquid-liquid equilibria of pentafluoroethane and ionic liquid [bmim][PF₆] mixtures studied with the volumetric method. *J. Phys. Chem. B* **2006**, *110*, 14436–14443.
- (38) Shiflett, M. B.; Yokozeki, A. Vapor-Liquid-Liquid equilibria of hydrofluorocarbons + 1-butyl-3-methylimidazolium hexafluorophosphate. *J. Chem. Eng. Data* **2006**, *51*, 1931–1939.
- (39) Lemmon, E. W.; McLinden, M. O.; Huber, M. L. Standard Reference Data Program. *REFPROP*, version 8.0; National Institute of Standards and Technology: Gaithersburg, MD, 2008.
- (40) Fernandez, A.; Garcia, J.; Torrecilla, J. S.; Oliet, M.; Rodriguez, F. Volumetric, transport and surface properties of [bmim][MeSO₄] and [emim][EtSO₄] ionic liquids as a function of temperature. *J. Chem. Eng. Data* **2008**, *53*, 1518–1522.
- (41) Yokozeki, A.; Shiflett, M. B. Global phase behaviors of trifluoromethane in ionic liquid [bmim][PF₆]. *AIChE J.* **2006**, *52*, 3952–3957.
- (42) Yokozeki, A.; Shiflett, M. B. Separation of Carbon Dioxide and Sulfur Dioxide Gases Using Room-Temperature Ionic Liquid [hmim][Tf₂N]. *Energy Fuel* **2009**, *23*, 4701–4708.
- (43) Van Ness, H. C.; Abbott, M. M. *Classical Thermodynamics of Nonelectrolyte Solutions*; McGraw-Hill: New York, 1982.
- (44) Span, R.; Wagner, W. A new equation of state for carbon dioxide covering the fluid region from the triple-point temperature to 1100 K at pressures up to 800 MPa. *J. Phys. Chem. Ref. Data* **1996**, *25*, 1509–1596.
- (45) Shiflett, M. B.; Yokozeki, A. Chemical absorption of sulfur dioxide in room-temperature ionic liquids. *Ind. Eng. Chem. Res.* **2010**, *49*, 1370–1377.
- (46) van Konynenburg, P. H.; Scott, R. L. Critical Lines and Phase Equilibria in Binary Van Der Waals Mixtures. *Philos. Trans. R. Soc. London A* **1980**, *298*, 495–540.
- (47) Yokozeki, A.; Shiflett, M. B. Hydrogen purification using room-temperature ionic liquids. *Appl. Energy* **2007**, *84*, 351–361.
- (48) Yokozeki, A.; Shiflett, M. B. Binary and ternary phase diagrams of benzene, hexafluorobenzene, and ionic liquid [emim][Tf₂N] using equations of state. *Ind. Eng. Chem. Res.* **2008**, *47*, 8389–8395.
- (49) Peng, X.; Wang, W.; Xue, R.; Shen, Z. Adsorption separation of CH₄/CO₂ on mesocarbon microbeads: Experiment and modeling. *AIChE J.* **2006**, *52*, 994–1003.
- (50) Rowlinson, J. S.; Swinton, F. L. *Liquids and Liquid Mixtures*, 3rd ed.; Butterworth: London, 1982.
- (51) Huang, X.; Margulis, C. J.; Li, Y.; Berne, B. J. Why is the partial molar volume of CO₂ so small when dissolved in a room temperature ionic liquid? Structure and dynamics of CO₂ dissolved in [Bmim+][PF₆⁻]. *J. Am. Chem. Soc.* **2005**, *127*, 17842–17851.

Received for review April 22, 2010. Accepted July 1, 2010. The authors thank DuPont Central Research and Development for supporting this work.

JE1004005